

Ion-Implantation-Related Atomic Collision Studies At The ORNL Multicharged Ion Research Facility

F. W. Meyer, M. E. Bannister, C. C. Havener, H. F. Krause, P. Krstic,
D. R. Schultz, A. Agarwal¹, D. Swenson^{1*}, F. Yan²

Physics Division, Oak Ridge National Laboratory, Oak Ridge, TN 37831-6372

¹*Axcelis Technologies, Beverly, MA*

²*Plasmaco Inc., Highland, NY*

Abstract. In this article, some atomic collision data needs in the ion-implantation industry are discussed, and illustrated by specific examples of electron impact and heavy particle cross sections measured or calculated in our atomic collisions group for ion source modeling, beam energy contamination determination, and wafer dose error corrections. An example is also provided of how ion implantation has been used in our laboratory to investigate ways of improving the operating characteristics of ac plasma display panels.

INTRODUCTION

Ion implantation [1] is a critical technology in forming all doped regions of modern integrated circuit (IC) structures. B or In ion beams are used for creation of p-type doped regions, while P, As, or Sb beams are used to create regions of n-type doping. Required beam energies cover an extremely wide range. On one extreme, the continuing decrease of the lateral dimensions of complimentary metal oxide semiconductor (CMOS) devices to achieve speed improvements requires a corresponding decrease of vertical dimensions. Thus, ultra-shallow doping for gate profiling and creating source/drain regions requires beam energies down to about 100 eV. There is also increasing use of higher implantation energies for, e.g. modulated wells for CMOS formation, requiring ~200 keV, retrograde wells utilizing implant energies up to 1.5 MeV, and triple wells for flash memory and high dose buried layers, performed at implant energies extending to several MeV.

While traditionally three types of implantation machines have been required to cover this broad energy range, new generations of ion sources and implanters are under development with wider energy range capabilities, to reduce the number of required implantation systems and thus overall production cost. Wafer biasing, either decel or accel, is being explored to extend the energy range of implanter machines. In addition, the use of multicharged dopant ions is contemplated to extend high energy

* Present address: Epion Corp., Billerica, MA

capabilities, while dimer, trimer, and cluster dopant ions (the latter based, e.g., on $B_{10}H_{14}$ source gas [2]) are being increasingly used for low energy applications.

As is well documented by now, the performance improvement of semiconductor devices continues to proceed at an incredible pace [3,4]. These improvements impose ever-increasing constraints on all aspects of the implantation process. Of particular relevance to the present article are the tolerances on ion beam energy contamination and wafer dose errors, which are now less than 1%.

Continuation of performance improvements on the present pace will be possible only with a significant evolution in process control methodology (see the *International Technology Roadmap for Semiconductors: 2001*, Ref. [5]). Whereas a largely empirically based (i.e., trial and error) approach to optimization of semiconductor processing technology has sufficed in the early days, a gradual change to a more phenomenological approach has occurred in recent years. Continuing along this trend, future optimization will have to rely increasingly on model-based approaches that require basic physics understanding of the relevant processes in order to enable real time process control, and to permit predictive simulation and exploration of new, as yet unexplored, operating regimes and conditions.

Efforts have been undertaken to make the transition to basic physics understanding in a number of semiconductor processing areas. Among them are implantation ion source modeling, estimation of implantation beam energy contamination, and wafer dose correction. In the following three sections, some of the atomic collision data requirements arising from such endeavors are highlighted using cross sections measured at the ORNL Multicharged Ion Research Facility (MIRF) [6] or calculated in-house by CFADC/Theoretical Atomic physics for Fusion [7] personnel. In the final section, work carried out at ORNL MIRF is described illustrating an alternate application of ion implantation, namely in the improvement and optimization of plasma display panels. The work also highlights an alternate approach to device optimization via a small test bench where the global effects of parameter changes can be conveniently evaluated. The work described below has in large part been carried out under the auspices of the US DOE Laboratory Technology Research Program, and under a Work for Others (WFO) contract with Eaton Semiconductor Corp. (now Axcelis Technologies, Inc.), who own the intellectual property rights to some of the data highlighted below.

IMPLANTATION ION SOURCE MODELING DATA NEEDS

For the reasons mentioned in the previous section, there is appreciable interest in assessment of possible optimization for multicharged ion production of Bernas and ELS hot cathode ion sources [8] presently used for singly charged ion production. The use of multicharged ions for higher energy ion implantation operations presents significant cost savings since the same acceleration facilities already in place for singly charged ion implantation could be used, while extending the maximum implantation energy by factors of two or three, depending on extracted charge state. Whether the same ion source can be used as well, will depend on the beam intensities that can be produced for the desired multiply charged ion. Knowledge of the relevant electron and heavy particle impact inelastic cross sections is required to guide the

range of arc voltages and source pressures to explore, since those two parameters are the main determinants of the electron energy distributions in the above ion sources.

Some of the atomic collision cross sections relevant to an implantation ion source plasma based on BF_3 source gas were determined as part of a WFO project for Eaton Semiconductor Corp. (now Axcelis Technologies, Inc). The goal of the latter was to lay the groundwork for quantitative ion source plasma modeling which would enable prediction of the source conditions giving the required boron beam properties as well to facilitate source optimization of multicharged B ion production for use in next generation micro-electronic devices. Most of the collision cross sections for a BF_3 plasma were until recently unknown.

At the ORNL Physics Division MIRF, unique apparatus exists for the measurement of such collision cross sections. This includes a state-of-the art electron cyclotron resonance (ECR) [6] ion source for producing singly and multiply charged B and F ions, as well as the many singly charged radicals formed from neutral BF_3 ; an electron crossed beam apparatus for measuring electron impact ionization and dissociation cross sections; and a beam - gas cell set-up for measuring many of the heavy particle charge exchange and dissociation cross sections of interest. To complement and extend the experimental work, theoretical estimates were made of the relevant electron-neutral collision cross sections, as well as of the heavy particle cross sections from the ~ 200 eV minimum energies experimentally accessible with the present set-up down to the 5-30 eV energy required for the source plasma modeling.

Selected Cross Section Results

One of most important class of collisions in low temperature plasmas is collisions with electrons. Using known scalings, comparisons with similar systems, additivity theorems, and semi-empirical relations, theoretical cross section estimates were made for electron impact ionization of BF_3 , as well as the major dissociation channels. In addition, measurements were performed of electron impact ionization of B^{q+} and F^{q+} , ions ($q = 1-3$) in the energy range 0-200 eV, and of the following electron fragmentation cross sections in the energy region 1-100 eV:

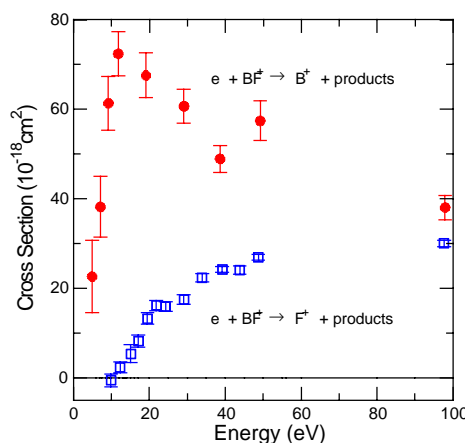
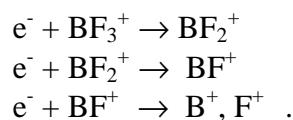
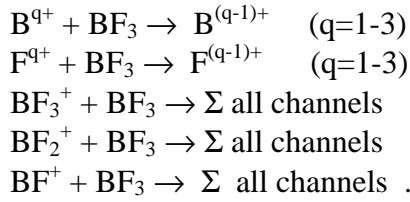


Figure 1. Electron impact fragmentation of BF^+



Another important class of collisions taking place in low temperature plasmas are heavy particle charge exchange and dissociation. For example, charge exchange collisions provide the dominant recombination process that determines mean charge states of extracted ions. In-house experimental apparatus for measuring heavy particle collision cross sections was used for the determination of

charge exchange and total attenuation cross sections at collision energies down to about 200 eV in energy:



By “ Σ all channels” is meant the sum of charge exchange and overall dissociation cross sections, i.e. total attenuation. In conjunction with the heavy particle collision

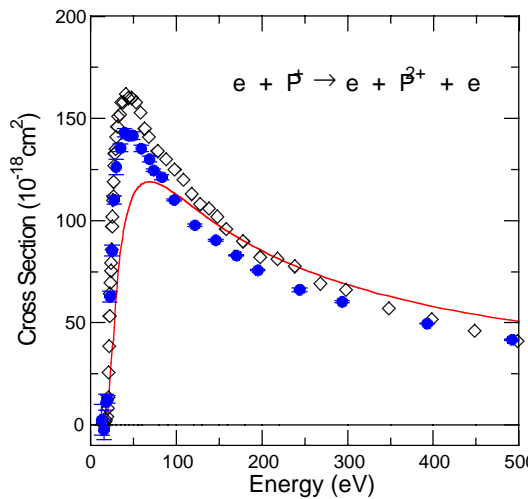


Figure 2. Electron impact ionization of P^+ : open symbols - Ref. 9; solid line - Lotz [10], solid symbols – present data

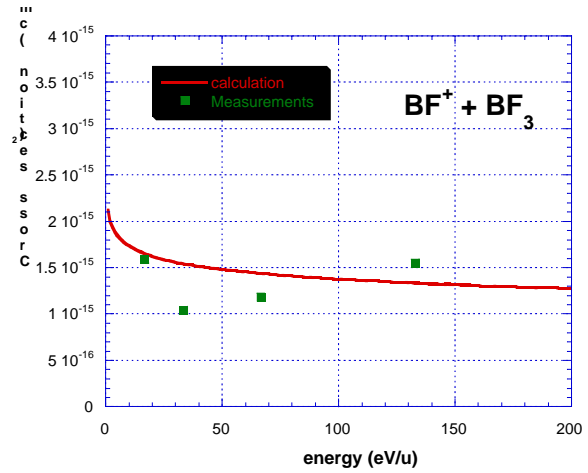


Figure 3. Experimental attenuation cross section compared with estimated single electron capture cross section for BF^+ in BF_3 .

cross section measurements, theoretical estimates based on Demkov or Landau-Zener models of non-adiabatic coupling were made to guide extrapolation down to the energies relevant for ion source modeling. The total experimental uncertainties of the cross section measurements are estimated to be at the 20% level . A measurement of a previously published electron capture cross section [11] for $O^{3+} + H_2 \rightarrow O^{2+}$ obtained with completely different apparatus agreed to within 3% of the published value. Figures 1-3 show sample cross section results for electron impact ionization, fragmentation, and heavy particle charge exchange.

Boron Beam Development With The MIRF ECR Source

As already mentioned earlier, the development of intense multicharged B ion beams is of great interest to the ion implantation industry because it cheaply extends the energy range of current ion implanters required for certain applications. The ORNL MIRF ECR ion source was used to investigate plasma conditions that optimized multicharged B ion production. For comparison, both BF_3 source gas and a solid B sample biased at negative voltage to enhance sputtering were investigated. The effect

of varying microwave power levels, source magnetic field configurations, source gas feed rates, and mix gas species on extracted beam charge state distributions was investigated and documented. Results for the biased B sample are summarized in the table below. Although not providing nearly as intense beams of multicharged ions as was achievable with BF_3 source gas, the biased B sample test provided an interesting insight into the mechanism whereby the solid B sample is converted to vapor. From the roughly proportional dependence of the extracted beam currents on sputter current under low microwave power conditions (i.e. B^+ ion production), the dominant mechanism is inferred to be simple sputtering. In contrast, at the high rf power conditions required for B^{2+} and B^{3+} production, the more exponential increase of the extracted currents with the power to the B sputter sample indicates a transition to sample evaporation, as the sample vapor pressure increases close to exponentially with temperature.

Although not documented here, ECR sources may prove to be better than the present Bernas ion implantation source for the production of B^{2+} and B^{3+} ion beams from BF_3 . For example, an all-permanent-magnet ECR ion source developed by Pantechnik [12] in Caen, France is currently producing almost a mA of B^{2+} , and more than 100_A of B^{3+} .

TABLE 1. Boron single and multicharged ion generation in the ORNL MIRF ECR source using a biased B sputter sample; 10 kV source high voltage; 5×10^{-6} Torr gauge reading for He sputter gas; I(mA) is sputter sample current; Beam(nA) is extracted ion beam current.

Bias voltage(V)	B^+ (54 W)		B^{2+} (254 W)		B^{3+} (254W)	
	I(mA)	Beam(nA)	I(mA)	Beam(nA)	I(mA)	Beam(nA)
250	10	15			0	0
500	12	40				
750	12	50				
1000	15	60	32	35	34	3
1250	15	70	36	90	37	50
1500	17	80	40	200	45	300
1750	18	93	45	650	49	750
2000	20	-	54	2000	51	1800

ENERGY-CONTAMINATION-RELATED CROSS SECTIONS

A common scheme for extending the range of energies and penetration depths obtained from any implantation equipment is to use multiply charged monatomic, or singly charged polyatomic ion species. However, the use of such species introduces the risk of having some energy contamination [13] in the beam, which ultimately results in a broadening of the implantation depth distribution. This risk arises because the other species are simultaneously emitted from the ion source. As an example, in a beam of doubly charged atomic ions, accelerated at a potential V, there can be a spurious component of singly charged monatomic ions which has 1/4 the kinetic energy per atom of the doubly charged ion, and therefore penetrate to a correspondingly smaller depth in the target material. The singly charged monatomic ion beam results from dissociation of singly charged diatomic ions with the background gas in the implanter beamline between ion source and analyzing magnet.

For instance, when implanting P^{2+} at 2 keV [1 kV/(unit charge)], the beam may be contaminated with P^+ at 0.5 keV, the latter having been accelerated through the 1-kV potential as P_2^+ and subsequently undergoing dissociation in the beamline residual gas preceding the analyzing magnet. Both species have the identical momentum per charge ratio, and so are not separated in the analyzing magnet. To address this issue, cross section measurements and calculations were made of simple dissociation and total attenuation of As_2^+ and P_2^+ colliding with H_2 , and CH_4 gases at keV energies. Experimental results for As_2^+ are shown in Table 2.

TABLE 2. Dissociation and total attenuation cross sections for As_2^+ ions in H_2 and CH_4 gases.

Energy (keV)	H_2		CH_4	
	-diss (10^{-16} cm^2)	-att (10^{-16} cm^2)	-diss (10^{-16} cm^2)	-att (10^{-16} cm^2)
3.0	1.8	3.3	2.1	11
5.0	3.4	4.1	3.0	13

As an additional example, in a beam of singly-charged diatomic ions, accelerated across a potential V , there can be a spurious component of singly-charged atomic ions which have 4 times the kinetic energy per atom of the diatomic ion, and therefore penetrate to a correspondingly greater depth in the target material. The singly charged atomic ion beam results from charge exchange of doubly charged atomic ions with the background gas molecules in the implanter beamline. For instance, when implanting P_2^+ at 1 keV (0.5 keV per atom), the beam may be contaminated with P^+ at 2 keV, produced from extracted P^{2+} that has undergone single electron capture prior to magnetic analysis. Ion implantation machine vendors must be able to specify for their customers the amount of energy contamination which

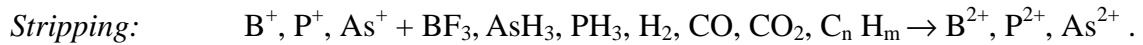
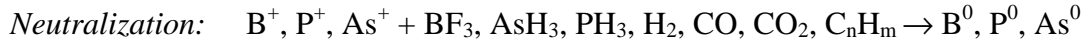
TABLE 3. Data summary of single electron capture cross section of B^+ , P^{2+} , and As^{2+} incident on various gases; (*) denotes total attenuation cross section.

Projectile	Energy (keV)	Cross Section (10^{-16} cm^2)					
		H_2	CO	N_2	O_2	CH_4	CO_2
B^+	2.0		6.4			10.2	10.0
B^+	5.0	3.7	7.2	4.3		7.3	7.9
P^{2+}	4.0	24.1		26.1	18.4		
	6.0	22.7		23.6	18.3		
	10.0	17.4		20.9	18.0		
	20.0	16.9*		26.2*	21.0*		
	36.0	11.0*		18.7*	16.0*		
As^{2+}	4.0	11.8		11.6	13.7		
	6.0	11.5		11.8	15.1		
	10.0	10.7		11.4	17.9		
	20.0	7.9*		13.6*	15.6*		
	36.0	7.0*		12.8	17.8*		

will be present in any beam as a function of known or measurable equipment parameters such as the ion energy or the pressure and composition of the background gas in the beamline. The energy contamination can be predicted from the probability of charge exchange, characterized by the charge changing or dissociation cross section of the various ions with gases present in the beamline. Until recently, there was little

such data applicable to the ion species, energies, and gases used today in the microelectronics field. Most available data had been obtained in support of fusion energy research. Table 3 itemizes some sample cross section results.

Below is a more complete list of the processes needed to address energy contamination as well as the dose correction issues to be discussed in the next section.



The energies for which these cross sections are needed range from a hundred eV to a few MeV! With exception of selected cases in the range 3 – 36 keV, and the B^+ stripping cross section shown in the next section, these cross sections are for the most part not known.

Dose Correction related cross sections An additional problem that arises from charge exchange is accuracy of implant-dose measurement, which relies on integration

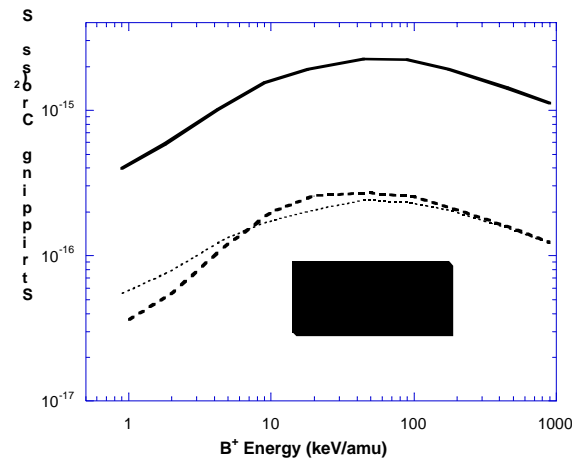


Figure 4. Stripping cross section for B^+ on BF_3 leading to B^{2+} .

capture in this section of beamline will not be detected at all when they reach the target, leading to an undercounting of the implantation dose. The cross sections of Table 2 and 3 are relevant for this issue as well, in the case of low energy implantation. In the case of high-energy implantation, stripping collisions prior to wafer impact but after magnetic analysis stage can similarly result in errors in dose estimation, leading to overestimation rather than underestimation of dose. A relevant cross section for this case is illustrated in Figure 4. The cross section shown was determined theoretically using a classical trajectory Monte Carlo (CTMC) approach

of the beam current at the target. In this case, the concern is charge exchange that occurs in the beamline section between the analyzing magnet and target. For instance, singly ionized species that undergo single electron

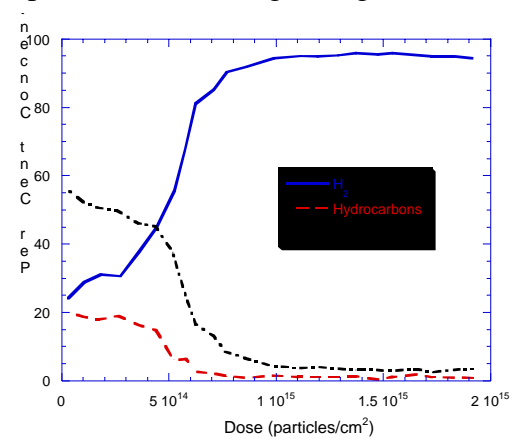


Figure 5. Evolution of the concentration of various outgassing species with accumulated dose for a 150 keV P implant.

under the assumption that the additivity rule applies, whereby the cross section for a molecular target is determined by a weighted sum of the cross sections of the constituent atoms, also shown in Fig. 4.

It is important to keep in mind that ion implantation occurs usually onto wafers with patterned photoresist coatings 1.5 – 4 μm thick. These coatings are usually organic in origin and respond to mA ion beam bombardment with significant outgassing, releasing a broad spectrum of gases ranging from H_2 , CO, and CO_2 , to a variety of hydrocarbons (CH_2 , CH_4 , and C_2H_2). This outgassing can raise the pressure in the wafer vicinity to as high as 10^{-3} Torr! Furthermore, as illustrated in Figure 5, the species released vary with accumulated dose, i.e. are time dependent [14]. These two features together make total dose estimation at the less than 1% level extremely challenging. Efforts are underway to implement real time partial pressure monitoring and species specific cross sections to extend the range of energies and pressures over which the robustness of present dose control algorithms can be maintained. The potential impact of photoresist outgassing on energy contamination is obviously most pronounced if wafer biasing is used, but may affect upstream (i.e. before magnetic analysis) energy contaminating collisions as well. Thus implanters almost universally require high pumping speed in the wafer vicinity and excellent differential pumping with respect to the upstream injection line.

OTHER IMPLANTATION APPLICATIONS

While dopant ion implantation has by far the biggest commercial usage, we highlight here briefly another application in the area of plasma display panels, a cutaway sketch of which is shown in Figure 6. Optimization of the top insulating coatings used in the construction of ac type Plasma Display Panels (PDP's) is presently an area of intense research. Choice of the coating material is critical to the operating voltage and lifetime of the plasma display panel. MgO has been empirically found to be an excellent coating material, resulting in desirable low operating voltages and long panel lifetimes [15]. This is presumably due to the high secondary electron

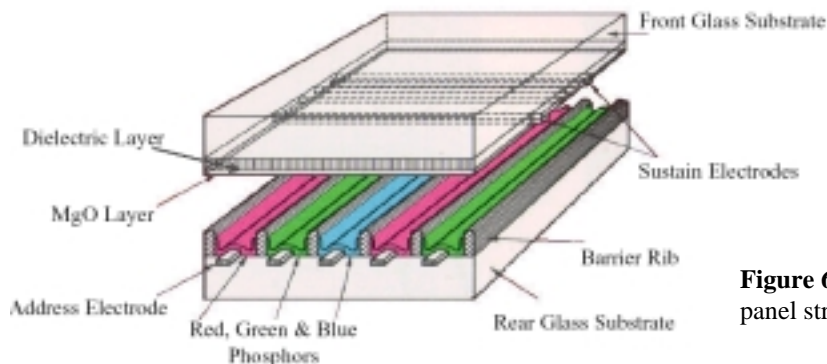


Figure 6. Color plasma display panel structure

emission and low sputtering rate properties of this material. As a possible aid in further improvements of device design, we have investigated the feasibility of using slow highly charged ions to modify MgO thin films. Any increases in secondary

electron emission can help reduce the operating voltage of a PDP and thus reduce the cost of the electronics (almost half of the cost of a PDP) and boost the luminous efficiency of the device. Reduced sputtering will increase panel lifetime, and thereby its competitiveness relative to other display types.

One possible mechanism that might enhance the secondary electron emission properties of the MgO thin film, is the creation of surface states close to the top of the 9.2 eV bandgap of the material by near-surface implantation of highly charged ions (HCI). If the implantation sufficiently distorts the local lattice, those local lattice defects may trap electronic excitations sufficiently long to provide a stepping stone for electrons leaving the surface, effectively enhancing the secondary electron emission yields. Alternatively, by suitable choice of species, the near-surface implanted HCI may themselves provide electronic states lying energetically between the MgO valence band and the vacuum, thus effectively lowering the threshold energy required for secondary electron emission, and thereby increasing electron yield. The latter scenario may also serve to reduce the priming time of such devices, which is essentially the discharge formation time delay. Reduction of this delay might alter the time budget of the pixel addressing sufficiently to enable increase of the number of addressing layers of the device, and is thus also of great interest.

The overall effect of near-surface implantation of MgO is of course extremely complex and difficult to disentangle in terms of the affected atomic and solid state processes. For this reason an approach using a mini-plasma display test panel developed at Plasmaco was employed which incorporates extensive diagnostics of the relevant display parameters and permitted almost real-time testing of the implantation regimen. This test stand

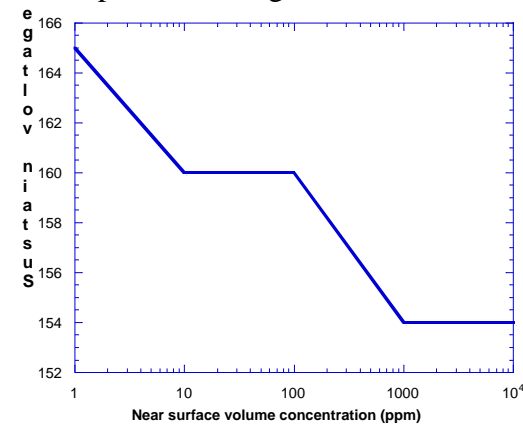


Figure 8. Dependence of measured sustain voltage on near-surface concentration of implanted Al.

back to Plasmaco. Energies were in the 10 keV range to result in depth distributions that peaked (see Fig. 7) at less than 100 Å according to SRIM 2000 [16]. The exposed samples were specifically evaluated for changes in sustain voltage, luminosity, and



Figure 7. SRIM 2000 simulation of implantation depth distribution for 10 keV Ni incident on MgO.

employs easily removable microscope-slide size lead glass substrates onto which mini-electrode arrays were deposited, which in turn were coated with a thin MgO layer. A set of such slides was implanted by various doses (representing near surface concentrations of 10 to 10⁴ ppm) of Al, Fe, Ni, and Cl ion beams at the ORNL MRF, and then evaluated in the test stand for possible performance improvements after transport

priming time. In this manner conditions (i.e. beam species, energy, and dose) that gave maximum display panel performance improvements could be immediately identified.

The MgO samples were mounted on a sample stage that could be heated up to 300° C to outgas the samples prior to implantation. The sample stage was designed to accommodate up to 4 15x50mm MgO samples to permit maximum throughput. A low energy electron flood gun was used to prevent sample charging during HCI beam exposure. In addition, a set of horizontal and vertical sweep plates was used to assure uniform illumination of the entire 7x20 mm active area of the MgO thin film.

Figure 8 summarizes the change in sustain voltage observed as function of the near-surface concentration of implanted 10 keV Al. As can be seen from the figure, an almost 10% decrease was observed. A 50% improvement in priming performance was noted for 10 keV Al implantation as well. The improvement of both parameters appears to peak at concentrations near the 1000-ppm level. These results show sufficient promise that further implantation runs are planned in the near future.

ACKNOWLEDGMENTS

This research was sponsored in part by the Office of Fusion Energy Sciences and by the Office of Science Laboratory Technology Research Program of the U.S. Department of Energy under contract No. DE-AC05-00OR22725 with UT-Battelle, LLC.

REFERENCES

1. McKenna, C. M., "History of Ion Implantation Equipment," in *Ion Implantation Science and Technology, 2000 Edition*, edited by J. F. Ziegler, Edgewater, Maryland: Ion Implantation Technology Co., 2000, pp. 1-45.
2. Sosnowski, M., et al., *Mat. Res. Soc. Symp. Proc.* **568**, 49 (1999).
3. Moore, Gordon E., *Electron.* **38**, 114_117 (April 19, 1965).
4. Isaac, R. D., *IBM J. Res. Develop.* **44**, 369 (2000).
5. see, e.g., <http://public.itrs.net/>
6. Meyer, F. W., "ECR-based Atomic Collision research at the ORNL MIRF," in *Trapping Highly Charged ions: Fundamentals and Applications*, edited by J. Gillaspay, Huntington, New York: Nova Science Publishers, Inc., 1997, pp. 117-165.
7. See, e.g. <http://www-cfadc.phy.ornl.gov>
8. Stephens, K. G., "Ion Source Physics," op.cit. ref [1], pp. 413-456.
9. Yamada et al., *J. Phys. Soc. Japan* **58**, 1585 (1999)
10. Lotz W., *Astrophys. J. Suppl.* **14**, 207 (1967); *Z. Phys.* **216**, 241 (1968); *Z. Phys.* **220**, 466 (1969).
11. Phaneuf, R. A. et al., *Phys. Rev. A* **26**, 1892 (1982).
12. See, e.g. <http://www.pantechnik.net>
13. Freeman, J. H., Chivers, D. J., and Gard, G. A., *Nucl. Instr. Meth.* **143**, 99 (1977).
14. Horsky, T. N., "Photoresist Outgassing in High Energy and High Current Ion Implantation," in *1998 Int. Conf. on Ion Implantation Proceedings*, Kyoto, Japan, June 22-26, 1998, p. 654.
15. Weber, L., "Color Plasma Displays", in *The Electrical Engineering Handbook*, CRC Press, pp. 1939 – 1950, 1997.
16. See, e.g., <http://www.srim.org/SRIM/SRIMLEGL.htm>